IEEE Access
Multidisciplinary | Rapid Review | Open Access Journal

Received September 13, 2019, accepted October 5, 2019, date of publication October 16, 2019, date of current version November 12, 2019.

Digital Object Identifier 10.1109/ACCESS.2019.2947673

Microwave Photonic Channelizer Based on Polarization Multiplexing and Photonic Dual Output Image Reject Mixer

CHENXU XIE, DAN ZHU, (Member, IEEE), WENJUAN CHEN, AND SHILONG PAN, (Senior Member, IEEE)

Key Laboratory of Radar Imaging and Microwave Photonics, Ministry of Education, Nanjing University of Aeronautics and Astronautics, Nanjing 210016, China

Corresponding authors: Dan Zhu (danzhu@nuaa.edu.cn) and Shilong Pan (pans@nuaa.edu.cn)

This work was supported in part by the National Natural Science Foundation of China under Grant 61971222, in part by the Natural Science Foundation of Jiangsu Province under Grant BK20160082, in part by the Jiangsu Provincial Program for High-level Talents in Six Areas under Grant DZXX-030, and in part by the Fundamental Research Funds for Central Universities under Grant NE2017002 and Grant NC2018005.

ABSTRACT Microwave photonic channelizer based on coherent frequency combs (OFCs) enables processing of ultra-wideband RF signals using low-frequency components. The channel number usually equals to the comb line number of the OFCs and the bandwidth for the microwave input is determined by the frequency spacing of the OFCs. However, the generation of coherent OFCs with large comb lines and large frequency spacing is extremely challenging, limiting greatly the potential of the OFC-based channelizer. In this paper, a microwave photonic channelizer based on polarization multiplexing and photonic dual output image reject mixing is proposed and demonstrated. A broadband signal can be divided into 8 channels using only one optical carrier and a pair of dual-polarization local oscillators (DP-LOs). Each DP-LO has only 2 spectral lines with orthogonal polarization states. In addition, by introducing a pair of OFCs with N comb lines, $8N$ channels can be output. The requirement of the comb line number is efficiently reduced, and the in-band interference is greatly suppressed by introducing the polarization multiplexing and the photonic dual-output image-reject mixing. A proof-of-concept experiment is carried out. An RF signal with 9.6-GHz bandwidth centered at 14 GHz is successfully divided into 8 channels with 1.2-GHz bandwidth, and the in-band interference is effectively suppressed for each channel. In addition, RF signals with 2.4-GHz bandwidth centered at 24.8 and 30.8 GHz are also successfully channelized, respectively.

INDEX TERMS Microwave photonics, optical polarization, frequency conversion.

I. INTRODUCTION

Microwave photonic channelization has been widely studied in recent years, due to the wideband RF signal processing capability which is urgently required in modern RF systems [1]–[4], including radar, electronic warfare, satellite payload and so on. The microwave photonic channelization realizes the function of slicing a wideband RF signal into narrowband channels compatible with current electronics by introducing photonic technologies [5]–[15]. There are three main methods to realize the microwave photonic channelization. For the first one, the RF signal is modulated to the optical domain, which is then sliced into a number of channels through using optical filter arrays [5]–[7]. However, the requirement with the optical filters is strict, making the optical filters hard to realize. For the second method, the RF signal is copied to the comb lines of an optical frequency comb (OFC), which is then filtered by a periodic optical filter with a slightly different filtering period as compared with the comb line frequency spacing [8]–[11]. However, the detailed information is lost during the optical-to-electrical conversion because of the square-law detection. The third method is based on two coherent OFCs having slightly different comb line frequency spacings [12]–[14]. One OFC is used to broadcast the RF signal, while the other OFC is used to downconvert different components of the RF signal to the same intermediate frequency (IF) band at different channels. The two OFCs can also be equivalently realized by using linear frequency

The associate editor coordinating the review of this manuscript and approving it for publication was Weiren Zhu.

modulated optical pulses. The slightly different comb line spacings are realized by introducing proper time delays between the optical pulses, as proposed in [15]. However, for all the reported schemes, the channel number equals to the comb line number of the OFCs, and the bandwidth for the microwave input is determined by the frequency spacing of the OFCs. Thus, the requirement for the optical carrier number rapidly increases with the increasing of the channel number. Since the generation of coherent OFCs with large comb lines and large frequency spacing is extremely challenging, the potential of the OFC-based channelizer is greatly limited.

Recently, we have proposed a microwave photonic channelizer based on polarization multiplexing and photonic dual-output image-reject mixing [16]. Four channels can be produced with crosstalk greatly suppressed with only one optical carrier and two polarization-orthogonal photonic LOs. The number of the optical carriers is greatly reduced. An RF signal centered at 10 GHz with a 4.8-GHz bandwidth is successfully experimentally divided into 4 channels. However, only some preliminary experimental results were reported, which is insufficient to understand the approach in-depth.

In this paper, investigations in detail are performed on the microwave photonic channelizer based on polarization multiplexing and the photonic dual-output image reject mixing. Both the $+1^{\text{st}}$ and -1^{st} sidebands are used. A broadband signal is divided into 8 channels using only one optical carrier and a pair of dual-polarization local oscillators (DP-LOs). Each pair of DP-LOs has only 2 spectral lines with orthogonal polarization states. In addition, by introducing a pair of OFCs with N comb lines, $8N$ channels can be output. The requirement of the comb line number is efficiently reduced and the in-band interference is greatly suppressed by introducing the polarization multiplexing and the photonic dual-output image-reject mixing. A proof-of-concept experiment is carried out. An RF signal with 9.6-GHz bandwidth centered at 14 GHz is successfully divided into 8 channels with 1.2-GHz bandwidth, and the in-band interference is effectively suppressed for each channel. In addition, the flexibility and the high working frequency capability of the proposed microwave channelizer is also experimentally proved. RF signals with 2.4-GHz bandwidth centered at 24.8 and 30.8 GHz are also successfully channelized, respectively.

II. PRINCIPLE

The schematic diagram of the proposed microwave photonic channelizer is shown in Fig. 1(a). The optical carrier is divided into two parts. In the upper and lower branches, the optical carrier is frequency shifted by f_{s1} and f_{s2}, respectively. The frequency difference between f_{s1} and f_{s2} is $2f_{\mathrm{CH}}$, where f_{CH} is the channel bandwidth to be achieved. In the upper branch, the frequency shifted optical carrier is injected into a polarization-multiplexed dual-drive Mach-Zehnder modulator (PM-DMZM), at which single-tone RF signals of f_{LO1} and f_{LO2} are modulated with the double sideband modulation format. In this way, a pair of DP-LOs with orthogonal polarization states are obtained, as shown in Fig. 1(b). An optical filter is used to separate the pair of DP-LOs. The separated DP-LOs are sent to the LO ports of two 90° polarization-multiplexed optical hybrids, respectively. In the lower branch, the frequency-shifted optical carrier is modulated by the wideband RF signal with the double sideband modulation format, as shown in Fig. 1(b). The modulated optical signal is injected into an optical filter to separate the $\pm 1^{\text{st}}$ sidebands, which are then sent to the signal ports of the two 90° polarization-multiplexed optical hybrids, respectively. For each 90° polarization-multiplexed optical hybrid, the structure is shown in Fig. 1 (a), for which each optical input LO (signal) port has a polarization beam splitters (PBS) connected, respectively. The outputs of the PBSs are connected to two 90° optical hybrids, respectively. Thus, the two spectral lines of each DP-LO are polarization divided, while the optically carried sidebands are power divided. The expressions of the photonic LOs and the optically carried RF sidebands are as follows,

$$\begin{cases} E_{\mathrm{LO}m} = E_0 e^{j\omega_{\mathrm{LO}m}t} \\ E_{\mathrm{S}m} = E_0 \left(e^{j\omega_{\mathrm{SL}m}t} + e^{j\omega_{\mathrm{SR}m}t} \right) \end{cases} \tag{1}$$

where $\omega_{\mathrm{LO}m}$ represents the angle frequency of photonic LO_m, $\omega_{\mathrm{SL}m}$ and $\omega_{\mathrm{SR}m}$ represent the frequency components of the optically carried RF sideband located at the left and right sides of photonic LO_m as shown in Figs. 1 (c)-(f). Here, $m = 1, 2, 3, 4$ refers to the four 90° optical hybrids shown in Fig. 1 (a). The four optical outputs of each 90° optical hybrid are as follows

$$\begin{cases} E_{\mathrm{I1}m} = E_0 \left(e^{j\omega_{\mathrm{SL}m}t} + e^{j\omega_{\mathrm{SR}m}t} + e^{j\omega_{\mathrm{LO}m}t} \right) \\ E_{\mathrm{I2}m} = E_0 \left(e^{j\omega_{\mathrm{SL}m}t} + e^{j\omega_{\mathrm{SR}m}t} + e^{j\omega_{\mathrm{LO}m}t} \right) \\ E_{\mathrm{Q1}m} = E_0 \left(e^{j\omega_{\mathrm{SL}m}t} + e^{j\omega_{\mathrm{SR}m}t} + e^{j\omega_{\mathrm{LO}m}t} \right) \\ E_{\mathrm{Q2}m} = E_0 \left(e^{j\omega_{\mathrm{SL}m}t} + e^{j\omega_{\mathrm{SR}m}t} + e^{j\omega_{\mathrm{LO}m}t} \right) \end{cases} \tag{2}$$

The in-phase outputs ($E_{\mathrm{I1}m}$, $E_{\mathrm{I2}m}$) and the quadrature outputs ($E_{\mathrm{Q1}m}$, $E_{\mathrm{Q2}m}$) from each 90° optical hybrid are injected into the optical input ports of two balanced photo detectors (BPDs), respectively. The electric outputs of the BPDs can be expressed as

$$\begin{cases} i_{\mathrm{I}m} \propto 2\eta E_0^2 \left[\cos\left(\omega_{\mathrm{LO}m} - \omega_{\mathrm{SL}m}\right) t + \cos\left(\omega_{\mathrm{SR}m} - \omega_{\mathrm{LO}m}\right) t \right] \\ i_{\mathrm{Q}m} \propto 2\eta E_0^2 \left[-\sin\left(\omega_{\mathrm{LO}m} - \omega_{\mathrm{SL}m}\right) t + \sin\left(\omega_{\mathrm{SR}m} - \omega_{\mathrm{LO}m}\right) t \right] \end{cases} \tag{3}$$

where η represents the responsivity of the BPD. A 90° electrical hybrid is used to combine the outputs of the two BPDs. The two outputs of the 90° electrical hybrid are as follows

$$\begin{cases} i_{\mathrm{out1}m} = j \cdot i_{\mathrm{I}m} + i_{\mathrm{Q}m} = 4\eta E_0^2 \sin\left(\omega_{\mathrm{SL}m} - \omega_{\mathrm{LO}m}\right) t \\ i_{\mathrm{out2}m} = i_{\mathrm{I}m} + j \cdot i_{\mathrm{Q}m} = 4\eta E_0^2 \cos\left(\omega_{\mathrm{SR}m} - \omega_{\mathrm{LO}m}\right) t \end{cases} \tag{4}$$

As shown in Fig. 1, the frequency components of the optically carried RF sideband located at the left ($\omega_{\mathrm{SL}m}$) and the right ($\omega_{\mathrm{SR}m}$) sides of photonic LO_m are the image for

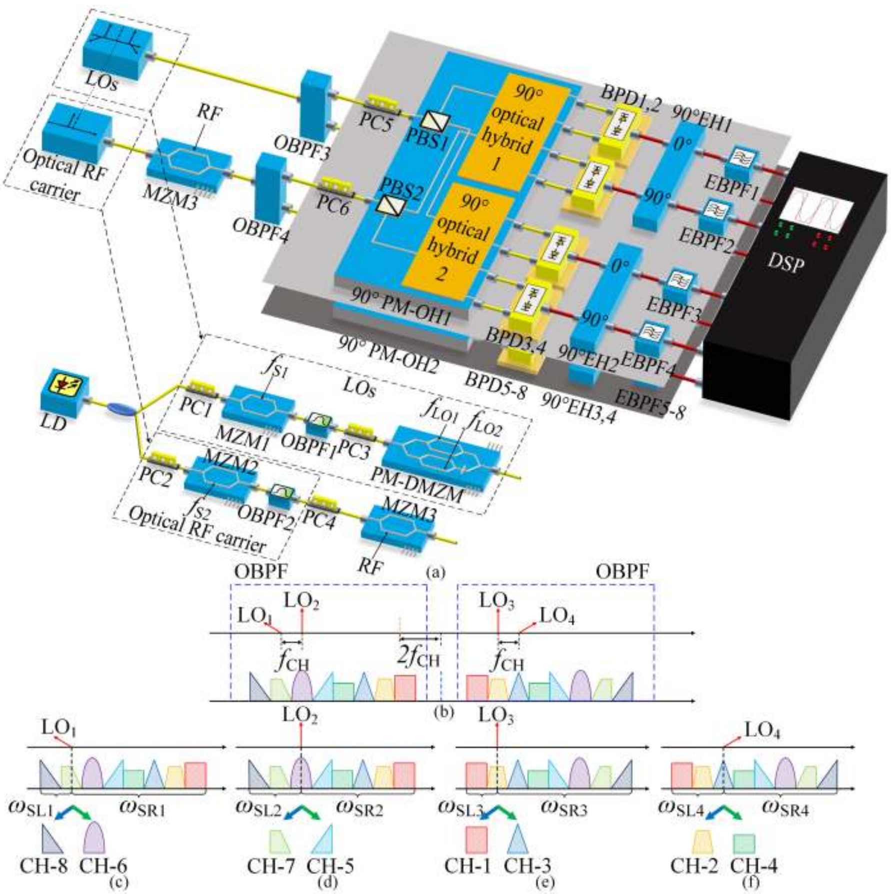

FIGURE 1. (a) Schematic diagram of the proposed microwave photonic channelizer based on polarization multiplexing and photonic dual-output image reject mixer. LOs: local oscillators; MZM: Mach-Zehnder modulator; RF: radio frequency; LD: laser diode; PC: polarization controller; OBPF: optical bandpass filter; PM-DMZM: polarization multiplexed dual drive Mach-Zehnder modulator; PC: polarization controller; 90° PM-OH: 90° polarization-multiplexed optical hybrid; PBS: polarization beam splitter; BPD: balanced photo detector; 90° EH: 90° electrical hybrid; EBPF: electrical band-pass filter; DSP: digital signal processor. (b) Spectra of the photonic LOs and the optically carried RF signal. (c)-(f) Spectra at the outputs of PBSs along the two orthogonal polarization axes of the 90° polarization-multiplexed optical hybrid.

each other. From Eq. 4, it can be seen that they are downconverted simultaneously, and output from the two output ports of the 90° electrical hybrid, respectively. Thus, two channels will be output with each photonic LO through introducing the microwave photonic dual-output image reject mixing based on the balanced Hartley structure [17]. In this way, with a pair of polarization-multiplexed photonic LOs shown in Fig. 1 (b), a microwave photonic channelization with eight channels will be realized. Only one optical carrier and a pair of DP-LOs composed of two polarization orthogonal spectral lines are used. The requirement of the photonic LO number is efficiently reduced, and the in-band interference is greatly suppressed by introducing the polarization multiplexing and the photonic dual-output image-reject mixing.

III. EXPERIMENTAL RESULTS AND DISCUSSIONS

An experiment is taken based on the schematic diagram shown in Fig. 1 (a). The optical carrier with a wavelength of 1550.52 nm and a power of 16 dBm is generated from a laser diode (LD, Teraxion PS-NLL-1550.52-080-000-A1). A 50:50 optical coupler is used to divide the optical carrier into two branches. In the upper branch, a 40-Gb/s Mach-Zehnder modulator (MZM1, FTM7938EZ) with the half-wave voltage of 3.5 V is driven by the single-tone signal of f_{s1} generated from an analog RF signal generator (Aglient E8257D, 200 KHz-67 GHz). An optical band-pass filter (OBPF1, Yenista XTM-50) is used to select one of the sidebands, realizing the frequency shift f_{s1} with the optical carrier. Then the optical carrier with frequency shift of f_{s1} is injected into a 40-Gbps PM-DMZM (FTM7980EDA) with the half-wave voltage of 3.5 V. Two sub-MZMs of the PM-DMZM are driven by two single-tone signals (f_{LO1} and f_{LO2}) generated from two analog signal generators (Keysight N5183B, 9 KHz-20 GHz; Anapico APSIN20G, 100 KHz-20 GHz), respectively. A pair of DP-LOs are generated at the output of the PM-DMZM. In the lower branch, MZM2 driven by a single-tone signal and OBPF2 are used to realize the frequency shift of f_{s2} with the optical carrier. The RF signal to be channelized is generated from an arbitrary waveform generator (AWG, Keysight M9502A, 65GSa/s), and applied to MZM3. OBPF3 (Yenista XTM-50) is used to separate the pair of DP-LOs, and OBPF4 (Yenista XTM-50) is used to separate the $\pm 1^{st}$ optically carried RF sidebands. Two 90° polarization-multiplexed optical hybrids (Kylia COH28) are used. The BPDs (Finisar BPDV2150R) have the working bandwidth of 41 GHz and the responsivity of 0.53 A/W. The 90° electrical hybrids (Pulsar QS8-13-463/7S) have the working frequency range of 0.5-10 GHz. A high-resolution optical spectrum analyzer (OSA, APEX AP2040D) with the resolution of 0.04 pm is used to measure the optical spectra. A signal analyzer (R&S FSV-40, 10 Hz-40 GHz) is used to measure the electrical spectra. The waveforms are observed with an oscilloscope (Keysight Infiniium DSOX93304, 80 GSa/s).

A. THE GENERATION OF PHOTONIC LOs

The single-tone signals with frequencies of 30 and 27.6 GHz are applied at MZM1 and MZM2, respectively. The optical carrier is frequency shifted by 30 and 27.6 GHz in the upper and the lower branches, respectively. In the upper branch, two single-tone LO signals with the frequencies of 13.4 and 14.6 GHz are applied to the PM-DMZM. The optical spectra at the output of the PM-DMZM is shown in Fig. 2 (a). A pair of DP-LOs are located at two sides of the frequency shifted optical carrier. The pair of DP-LOs are separated, with the optical spectra shown in Fig. 2 (b) and Fig. 2 (c), respectively. In order to verify that the two spectral lines for DP-LO_{1l} and DP-LO_{1r} are polarization orthogonal, the signal ports of the 90° polarization-multiplexed optical hybrids are disconnected. By tuning the PCs connected to the LO ports of the polarization-multiplexing 90° optical hybrids, the optical spectra at the two output ports of PBS1 along two orthogonal polarization axes are shown in Fig. 2 (d) and Fig. 2 (e), while the two outputs of PBS2 along two orthogonal polarization axes are shown in Fig. 2 (f) and Fig. 2 (g), respectively. It can be seen that the two spectral lines for each DP-LO are polarization orthogonal.

B. THE PERFORMANCE OF THE DUAL-OUTPUT MICROWAVE PHOTONIC IMAGE REJECT MIXING

Firstly, the image reject ratio (IRR) performance of the dual-output microwave photonic image reject mixing is experimentally measured. Photonic LO_3 shown in Fig. 2 (f) is used. Two RF signals with the same bandwidth of 1.2 GHz centered at 9.8 and 12.2 GHz are applied to MZM3, respectively, which are the image for each other. When the RF signal centered at 9.8 GHz (12.2 GHz) is used, the electrical spectra of the signals from the two output ports of 90° electrical hybrid1 are shown as the blue solid lines (red dashed lines) in Figs. 3 (a) and (b), respectively. As can be seen, the RF signals being image for each other are downconverted to the same IF band and output from the two output ports of the 90° electrical hybrid, respectively. The IRR at output port1 is 25 dB within the bandwidth of 1.2 GHz, while the IRR at output port2 is 21 dB within the bandwidth of 1.2 GHz.

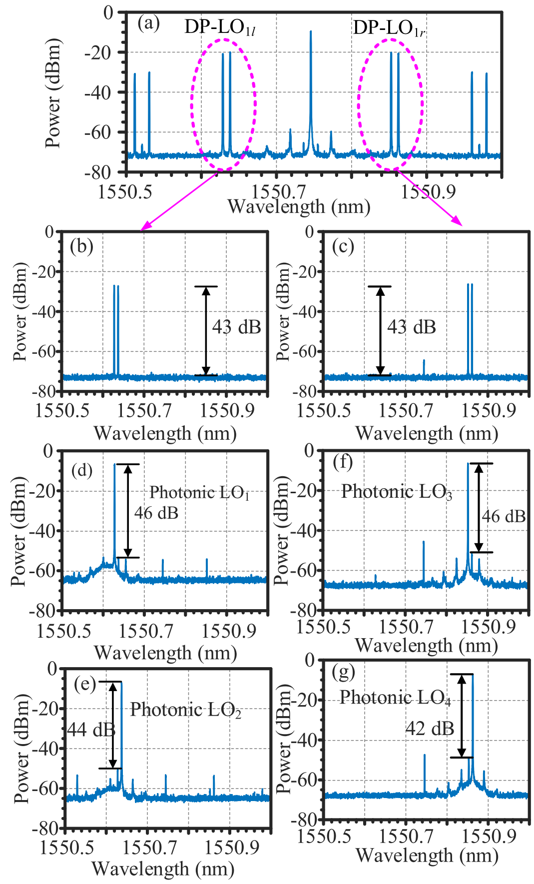

FIGURE 2. The experimentally observed optical spectra (a) at the output of the PM-DMZM; (b) the separated DP-LO_{1l}, (d) and (e) the orthogonally polarized output of DP-LO_{1l} split by PBS; (c) the separated DP-LO_{1r}; (f) and (g) the orthogonally polarized output of DP-LO_{1r} split by PBS. Here two single-tone LO signals with the frequencies of 13.4 and 14.6 GHz are applied to the PM-DMZM.

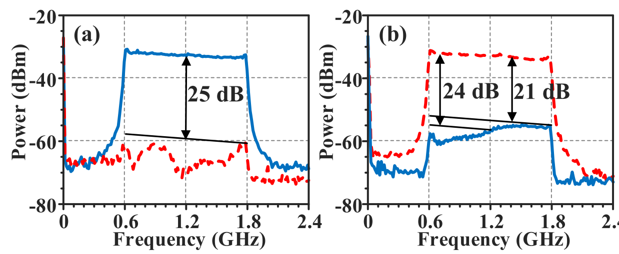

FIGURE 3. The experimentally observed electric spectra of signals at output ports of 90° electrical hybrid when the RF signals with the same bandwidth of 1.2 GHz and center frequency of 9.8 GHz (blue solid line) and 12.2 GHz (red dashed line) are applied to MZM3.

The phase and amplitude imbalances of the 90° electrical hybrid cause the performance difference between the two output ports. In this way, microwave photonic dual-output image reject mixing is realized. For each photonic LO, the frequency components being image for each other are downconverted and output simultaneously.

C. THE PERFORMANCE OF THE MICROWAVE PHOTONIC CHANNELIZER

An 8-channel channelization is realized by introducing the microwave photonic dual-output image reject mixing in each channel. A linear frequency modulated (LFM) signal with a 9.6-GHz bandwidth centered at 14 GHz to be channelized is applied to MZM3. The optical spectrum of the optically carried RF signal is shown as the blue solid line in Fig. 4, while the pair of DP-LOs generated in part A are shown as the red dashed line as a comparison.

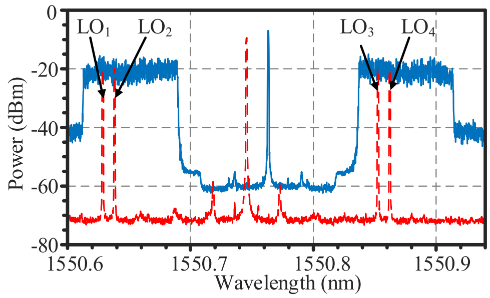

FIGURE 4. **The optical spectra of the pair of DP-LOs (red dashed line) and the optically carried RF signal with DSB modulation format (blue solid line). Here two single-tone LO signals with the frequencies of 13.4 and 14.6 GHz are applied to the PM-DMZM, and a LFM signal with a 9.6-GHz bandwidth centered at 14 GHz is used as the RF signal.**

The instantaneous frequency-time diagrams of the signals from the two output ports of 90° electric hybrid $i(i = 1, 2, 3, 4)$ are shown in Fig. 5 (a_i) and Fig. 5 (b_i), respectively. As can be seen, the optically carried RF sideband components located at the left and the right sides of the photonic LO_i are downconverted and output from the two output ports of 90° electric hybrid i, respectively. By using an electrical filter with passband of 0.6-1.8 GHz connected to each output port of the 90° electrical hybrids, the LFM signal with 9.6-GHz bandwidth centered at 14 GHz will be downconverted and sliced to 8 channels with 1.2-GHz bandwidth.

The instantaneous frequency-time diagrams of the output signals for the 8 channels are shown in Figs. 6 (a)-(h), respectively. Signals output from the 1st and the 3rd channels are downconverted from the 9.2-10.4 GHz and 11.6-12.8 GHz spectral slices of the RF signal with photonic LO_3, as shown in Figs. 6 (a) and (c), respectively. Similarly, signals from the 2nd and the 4th channels are downconverted from the 10.4-11.6 GHz and 12.8-14 GHz spectral slices of the RF signal with photonic LO_4, as shown in Figs. 6 (b) and (d), respectively. The 14-15.2 GHz and 16.4-17.6 GHz spectral slices are downconverted with photonic LO_2 and output from the 5th and the 7th channels, as shown in Figs. 6 (e) and (g), respectively. Meanwhile, the output signals from the 6th and the 8th channels are the downconverted results of the 15.2-16.4 GHz and 17.6-18.8 GHz spectral slices with photonic LO_1, as shown in Figs. 6 (f) and (h), respectively. Due to the symmetry of the negative frequency about zero as shown in Figs. 5 (a1)-(a4), the signals output from the 1st, 2nd, 5th, and 6th channels are down-chirped before digital signal processing.

It should be noted that in our experiments, the electrical filters are realized in digital domain. In addition, a frequency correction in digital domain is also applied to offset the frequency symmetry for the corresponding channels.

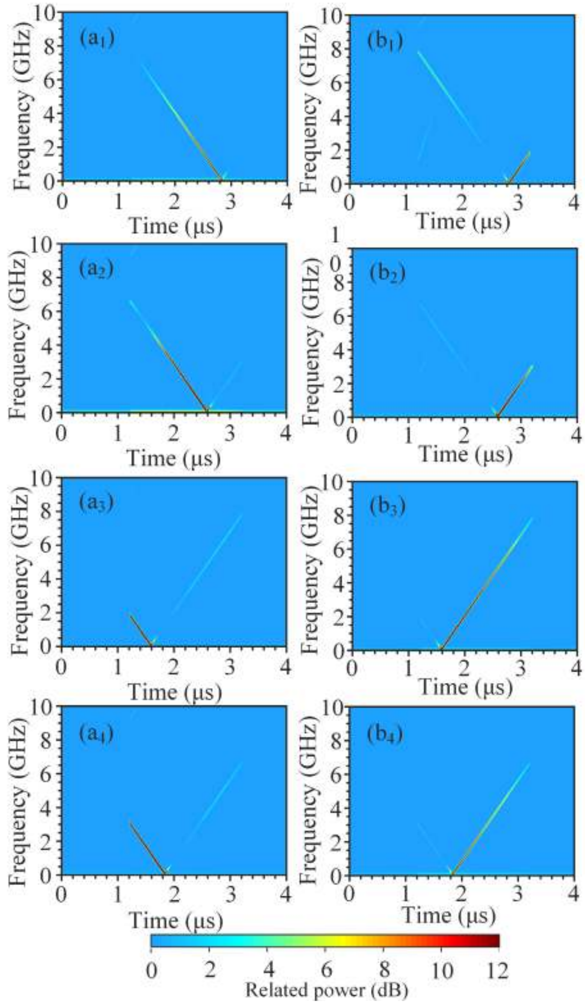

FIGURE 5. **The experimentally observed instantaneous frequency-time diagrams of the electrical signals from the output (a) port1 and (b) port2 of the 90° electrical hybrids 1-4, respectively, when a LFM RF signal with a 9.6-GHz bandwidth centered at 14 GHz is applied.**

Furthermore, a calibration is taken in digital domain to eliminate the imbalanced optical damage caused by the system itself. In our experiment, the input signal is a LFM signal that has the same amplitudes over the signal's bandwidth, thus here we mainly calibrate the amplitude responses of the channels. For an input signal that has more complicated format, a calibration process can be taken as follows: firstly, channelization is carried out with a known signal, and the amplitude, frequency and phase characteristics of the channelized output signal are compared with these of the initial input signal. In this way, the channel responses can be obtained, with which effective calibration of the channel responses can be implemented in digital domain.

D. THE FLEXIBILITY OF THE MICROWAVE PHOTONIC CHANNELIZER

In order to investigate the flexibility and the high working capability of the system, an up-chirped LFM signal with a bandwidth of 2.4 GHz centered at 24.8 GHz is

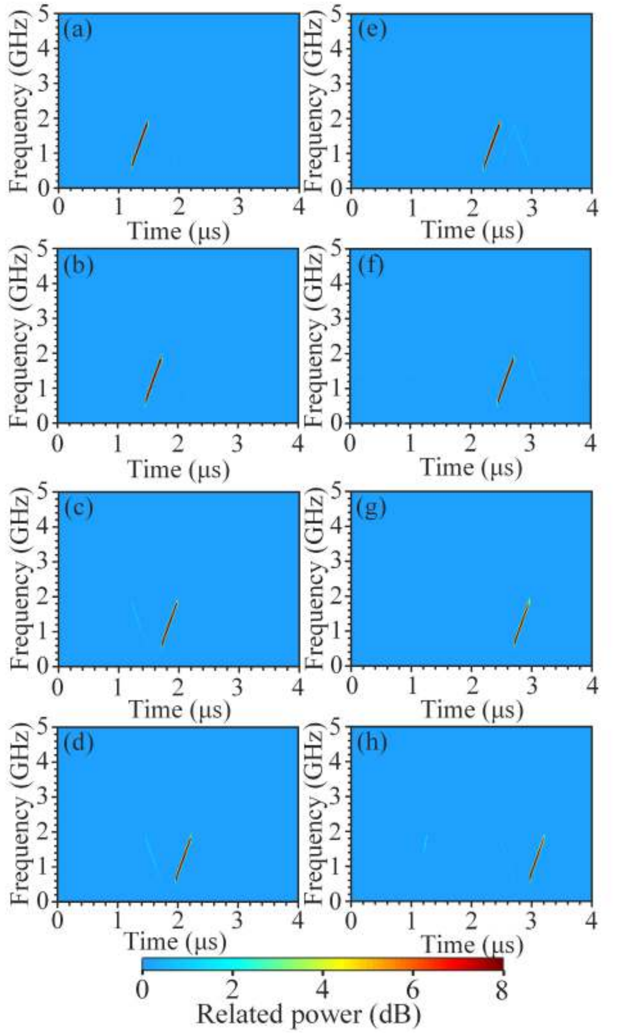

FIGURE 6. The experimentally obtained instantaneous frequency-time diagrams of signals output from the (a) 1st, (b) 2nd, (c) 3rd, (d) 4th, (e) 5th, (f) 6th, (g) 7th, and (h) 8th channels when a LFM RF signal with a 9.6-GHz bandwidth centered at 14 GHz is applied. It shows the successful channelization of 8 output channels with channel frequency range of 0.6-1.8 GHz.

applied to MZM3. Two single-tone signals with frequencies of 27.4 and 28.6 GHz are applied to the PM-DMZM. The frequencies of the signals applied to MZM1 and MZM2 are changed to be 18 and 15.6 GHz, respectively. The optical spectrum of the optically carried RF signal is shown as the blue solid line in Fig. 7, while the pair of DP-LOs are shown as the red dash line. Since the bandwidth of the LFM signal is only 2.4 GHz, only the $+1^{st}$ optically carried RF sideband and photonic LO_3 and LO_4 are needed to realize the channelization, with the detailed optical spectra given as the inset in Fig. 7. The instantaneous frequency-time diagrams of the downconverted signals are shown in Fig. 8 (a)-Fig. 8 (d). The signals at the 1^{st}- and 3^{rd}- channels are downconverted from the frequency slices of 23.6-24.4 GHz and 25.6-26 GHz with photonic LO_3, respectively. The 2^{nd} channel is downconverted from the frequency components of 24.4-25.6 GHz with photonic LO_4. In this way, the LFM signal with

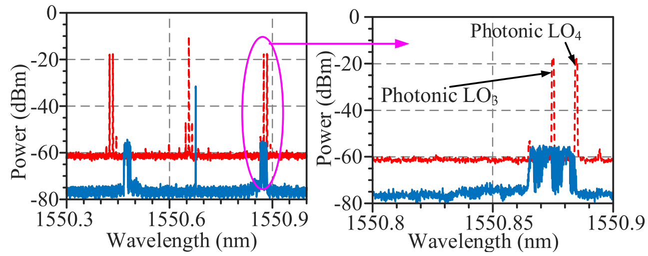

FIGURE 7. The experimentally observed optical spectra of the DP-LOs (red dashed line) and the optically carried RF signal with frequency range of 23.6-26 GHz (blue solid line). Inset: the detailed optical spectra of the right pair of DP-LO with two spectral lines and the $+1^{st}$ optically carried RF sideband.

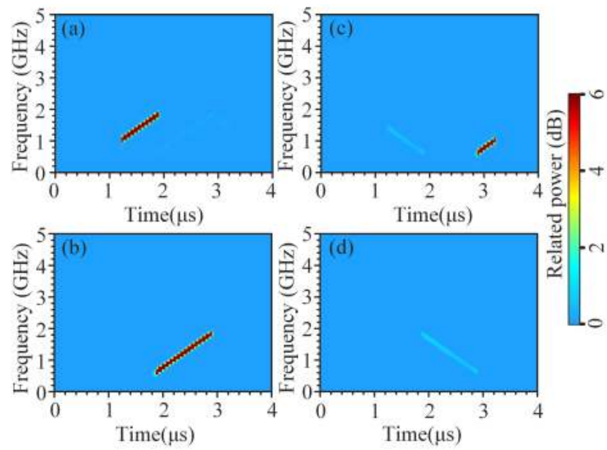

FIGURE 8. The experimentally obtained instantaneous frequency-time diagram of signals at the (a) 1st, (c) 3rd channel downconverted with photonic LO_3, and signals at the (b) 2nd, and (d) 4th channels downconverted with photonic LO_4 when a LFM signal with a bandwidth of 2.4 GHz centered at 24.8 GHz is applied.

2.4-GHz bandwidth centered at 24.8 GHz is successfully sliced to 3 channels.

Then the center frequency of the applied LFM signal is changed to be 30.8 GHz, and the spectra of the optically carried RF signal is shown as the blue solid line in Fig. 9. Only the -1^{st} optically carried RF sideband and photonic LO_1 and LO_2 are needed, with the optical spectra given in detail in Fig. 9. The LFM signal is successfully channelized,

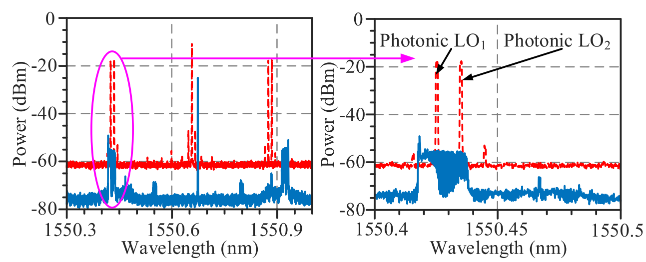

FIGURE 9. The experimentally observed optical spectra of DP-LOs (red dashed lines), optically carried RF signal with the frequency range of 29.6-32GHz (blue solid lines). Inset: the detailed optical spectra of the left pair of DP-LO with two spectral lines and the -1^{st} optically carried RF sideband.

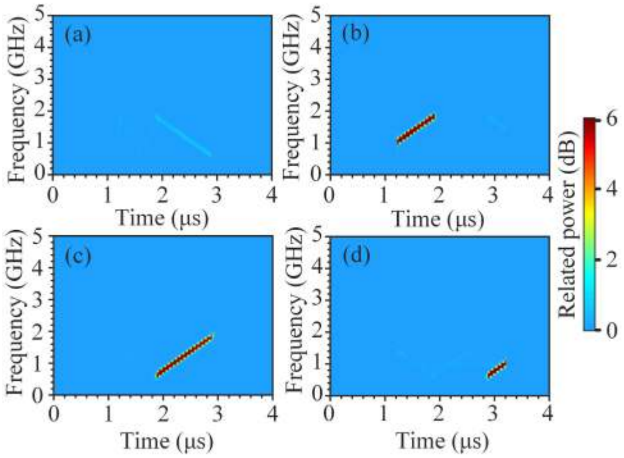

FIGURE 10. The experimentally obtained instantaneous frequency-time diagram of signals at the (a) 1st, (c) 3rd channel downconverted with photonic LO_2, and signals at the (b) 2nd, and (d) 4th channels downconverted with photonic LO_1 when a LFM signal with a bandwidth of 2.4 GHz centered at 30.8 GHz is applied.

with the instantaneous frequency-time diagrams of the output signals from each channel shown in Fig. 10 (a)-Fig. 10 (d), respectively. The 1^{st} channel outputs no frequency components. The 2^{nd} and the 4^{th} channels are downconverted with photonic LO_1 from the frequency components of 29.6-30.4 GHz and 31.6-32 GHz, respectively. In addition, the 3^{rd} channel outputs the downconverted component from the frequency component of 30.4-31.6 GHz. Thus, it can be seen that the proposed scheme has the capability to realize flexible channelization with up to 8 channels.

IV. DISCUSSION

In our experiment, 8 channels have been achieved with a pair of DP-LOs. The capability of the channelizer can be extended to $8N$ channels when a pair of OFCs (OFC1 and OFC2) are used as the optical sources as shown in Fig. 11 (a). The frequency of the k^{th} comb lines are follows

$$\begin{cases} f_{k,\mathrm{OFC1}} = f_{1,\mathrm{OFC1}} + (k-1)\,\Delta f_{\mathrm{OFC1}} \\ f_{k,\mathrm{OFC2}} = f_{1,\mathrm{OFC2}} + (k-1)\,\Delta f_{\mathrm{OFC2}} \end{cases} \tag{5}$$

where $f_{1,\mathrm{OFC2}} - f_{1,\mathrm{OFC1}} = 2f_{\mathrm{CH}}$ and $\Delta f_{\mathrm{OFC2}} - \Delta f_{\mathrm{OFC1}} = 4f_{\mathrm{CH}}, k = 1, 2, \ldots, N$, as shown in Fig. 11 (b). The frequency difference between the k^{th} comb lines of OFC1 and OFC2 is $(4k-2)f_{\mathrm{CH}}$.

In the upper branch, OFC1 is injected into the PM-DMZM to be modulated by two single-tone signals of f_{LO1} and f_{LO2} with the CS-DSB modulation format. In this way, a pair of DP-LOs are located at each comb line of OFC1, respectively, as shown in Fig. 11 (c). When the channelizer is used to realize the channelization of the frequency range of $[f_{\mathrm{L}}, f_{\mathrm{H}}]$, the frequency of f_{LO1} and f_{LO2} are set to be $f_{\mathrm{LO1}} = (f_{\mathrm{L}} + f_{\mathrm{H}} + f_{\mathrm{CH}})/2$, $f_{\mathrm{LO2}} = (f_{\mathrm{L}} + f_{\mathrm{H}} - f_{\mathrm{CH}})/2$, respectively. Thus, the frequencies of k^{th} pair of DP-LOs carried at the k^{th} comb line of OFC1 can be expressed as

$$\begin{cases} f_{k,1} = f_{1,\mathrm{OFC1}} + (k-1)\,\Delta f_{\mathrm{OFC1}} - f_{\mathrm{LO1}} \\ f_{k,2} = f_{1,\mathrm{OFC1}} + (k-1)\,\Delta f_{\mathrm{OFC1}} - f_{\mathrm{LO2}} \\ f_{k,3} = f_{1,\mathrm{OFC1}} + (k-1)\,\Delta f_{\mathrm{OFC1}} + f_{\mathrm{LO2}} \\ f_{k,4} = f_{1,\mathrm{OFC1}} + (k-1)\,\Delta f_{\mathrm{OFC1}} + f_{\mathrm{LO1}} \end{cases} \tag{6}$$

In the lower branch, OFC2 is modulated by the RF signal with the double sideband modulation format, as shown in Fig. 11 (c). The frequencies of the k^{th} pair of optically carried RF sidebands have the expression of

$$\begin{cases} f_{k,-1\mathrm{RF}} = f_{1,\mathrm{OFC2}} + (k-1)\,\Delta f_{\mathrm{OFC2}} - f_{RF} \\ f_{k,+1\mathrm{RF}} = f_{1,\mathrm{OFC2}} + (k-1)\,\Delta f_{\mathrm{OFC2}} + f_{RF} \end{cases} \tag{7}$$

Based on the principle proposed in part II, with the 1^{st} pair of DP-LOs and the 1^{st}pair of the optically carried RF sidebands, 8 channels of the $(4N-3)^{th}$ to the $(4N+4)^{th}$ will be output. Since the FSR difference Δf_{FSR} of the two OFCs equals to $4f_{\mathrm{CH}}$, the location of the k^{th} pair of DP-LOs moves of $4f_{\mathrm{CH}}$ to left being relative to the k^{th}pair of optically carried RF sidebands, as compared with the $(k-1)^{th}$ pair of DP-LOs being relative to the $(k-1)^{th}$ pair of optically carried RF sidebands, as shown in Fig. 12. Thus with the k^{th} pair of DP-LOs and the k^{th} pair of optically carried RF sidebands, 8 channels of the $(4N-4k+1)^{th}$ to the $(4N+4k)^{th}$ will be output. As shown in Fig. 12 (b), the frequency components down-converted by photonic $\mathrm{LO}_{k,1}$ is the $(4N+4k-2)^{th}$

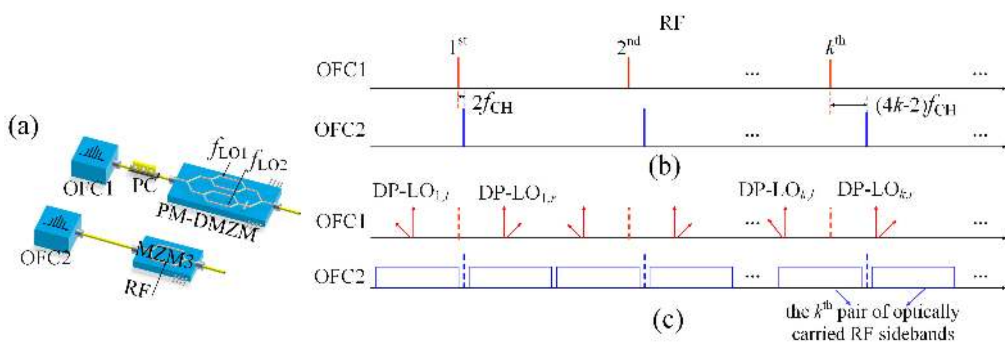

FIGURE 11. (a) Two OFCs introduced to extend the output channels of the proposed scheme. Here the two OFCs are used as the optical sources injected into the PM-DMZM and MZM3, respectively. OFC: optical frequency comb, (b) the comb lines of OFC1 and OFC2, (c) the optical spectra of OFC1 being modulated by two single-tone signals of f_{LO1} and f_{LO2} with the CS-DSB modulation format at the PM-DMZM, and the optical spectra of OFC2 being modulated by the RF signal with the double-sideband modulation format.

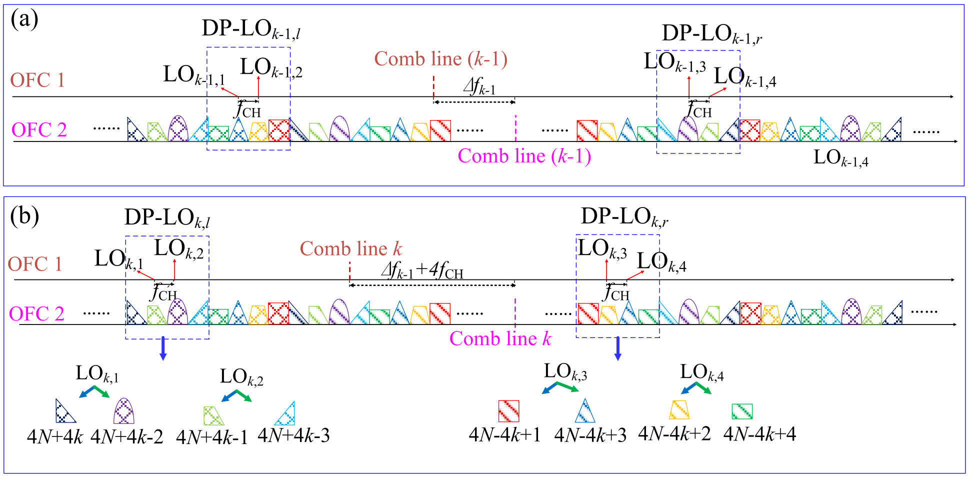

FIGURE 12. Schematic diagram of (a) the pair of DP-LOs and the pair of optically carried RF sidebands carried at the $(k-1)^{\text{th}}$ comb lines of OFC1 and OFC2, respectively, (b) the pair of DP-LOs and the pair of optically carried RF sidebands carried at the k^{th} comb lines of OFC1 and OFC2, respectively, and the output channels.

and $(4N+4k)^{\text{th}}$ channels. Similarly, the $(4N+4k-1)^{\text{th}}$ and $(4N+4k-3)^{\text{th}}$ channels are down-converted by photonic $\text{LO}_{k,2}$. The $(4N-4k+1)^{\text{th}}$ and $(4N-4k+3)^{\text{th}}$ channels are down-converted by photonic $\text{LO}_{k,3}$, and the $(4N-4k+2)^{\text{th}}$ and $(4N-4k+4)^{\text{th}}$ channels are down-converted by photonic $\text{LO}_{k,4}$. In this way, by introducing two pair of OFCs with N comb lines, a channelization with $8N$ channels is realized. In addition, with the development of integrated microwave photonics [18], [19], the proposed scheme can be integrated to be more compact and easy to be miniaturized and utilized.

V. CONCLUSION

A microwave photonic channelizer based on polarization multiplexing and photonic dual output image reject mixing is proposed and demonstrated. A broadband signal can be divided into 8 channels using only one optical carrier and a pair of DP-LOs composed of 2 spectral lines with orthogonal polarization states. In addition, by introducing a pair of OFCs with N comb lines, the proposed system can output $8N$ channels. The requirement of the comb line number is efficiently reduced, and the in-band interference is greatly suppressed by introducing the polarization multiplexing and the photonic dual-output image-reject mixing. A proof-of-concept experiment is carried out. An RF signal with 9.6-GHz bandwidth centered at 14 GHz is successfully divided into 8 channels with 1.2-GHz bandwidth, and the in-band interference is effectively suppressed for each channel. In addition, RF signals with 2.4-GHz bandwidth centered at 24.8 and 30.8 GHz are successfully channelized to 3 channels, respectively. The proposed scheme can find applications in RF systems with requirements to process wideband RF signals with high center frequencies, including radar, electronic warfare and so on.

REFERENCES

[1] P. Ghelfi, E. Lazzeri, F. Scotti, G. Serafino, A. Capria, S. Pinna, D. Onori, C. Porzi, M. Scaffardi, A. Malacarne, V. Vercesi, E. Lazzeri, F. Berizzi, and A. Bogoni, "A fully photonics-based coherent radar system," *Nature*, vol. 507, no. 7492, pp. 341–345, Mar. 2014.

[2] G. W. Anderson, D. C. Webb, A. E. Spezio, and J. N. Lee, "Advanced channelization for RF, microwave, and millimeterwave applications," *Proc. IEEE*, vol. 79, no. 3, pp. 355–388, Mar. 1991.

[3] S. Pan, D. Zhu, S. Liu, K. Xu, Y. Dai, T. Wang, J. Liu, N. Zhu, Y. Xue, and N. Liu, "Satellite payloads pay off," *IEEE Microw. Mag.*, vol. 16, no. 8, pp. 61–73, Sep. 2015.

[4] W. Namgoong, "A channelized digital ultrawideband receiver," *IEEE Trans. Wireless Commun.*, vol. 2, no. 3, pp. 502–510, May 2003.

[5] D. B. Hunter, L. G. Edvell, and M. A. Englund, "Wideband microwave photonic Channelised receiver," in *Proc. MWP*, Seoul, South Korea, Oct. 2005, pp. 249–252.

[6] S. Song, X. Yi, and T. Huang, "Microwave photonic channelized receiver based on double column microring array," in *Proc. OECC*, Shanghai, China, Jun./Jul. 2015, pp. 1–3.

[7] J. Wang, M. Chen, H. Yu, Y. Liang, H. Chen, S. Yang, and S. Xie, "Photonic-assisted seamless channelization based on integrated three-stage cascaded DIs," in *Proc. MWP*, Alexandria, VA, USA, Oct. 2013, pp. 21–24.

[8] X. Xu, J. Wu, M. Tan, T. G. Nguyen, S. T. Chu, B. E. Little, R. Morandotti, A. Mitchell, and D. J. Moss, "Broadband photonic RF channelizer based on micro-combs," *Proc. SPIE*, vol. 10917, Mar. 2019, Art. no. 1091722.

[9] X. Xie, Y. Dai, Y. Ji, K. Xu, Y. Li, J. Wu, and J. Lin, "Broadband photonic radio-frequency channelization based on a 39-GHz optical frequency comb," *IEEE Photon. Technol. Lett.*, vol. 24, no. 8, pp. 661–663, Apr. 15, 2012.

[10] X. Zou, W. Pan, B. Luo, and L. Yan, "Photonic approach for multiple-frequency-component measurement using spectrally sliced incoherent source," *Opt. Lett.*, vol. 35, no. 3, pp. 438–440, Feb. 2010.

[11] H. Huang, C. Zhang, H. Zhou, H. Yang, W. Yuan, and K. Qiu, "Double-efficiency photonic channelization enabling optical carrier power suppression," *Opt. Lett.*, vol. 43, no. 17, pp. 4073–4076, Sep. 2018.

[12] X. Xie, Y. Dai, K. Xu, J. Niu, R. Wang, L. Yan, and J. Lin, "Broadband Photonic RF channelization based on coherent optical frequency combs and I/Q demodulators," *IEEE Photon. J.*, vol. 4, no. 4, pp. 1196–1202, Aug. 2012.

[13] Z. Tang, D. Zhu, and S. Pan, "Coherent optical RF channelizer with large instantaneous bandwidth and large in-band interference suppression," *J. Lightw. Technol.*, vol. 36, no. 19, pp. 4219–4226, Oct. 2018.

[14] W. Chen, D. Zhu, C. Xie, J. Liu, and S. Pan, "Microwave channelizer based on a photonic dual-output image-reject mixer," *Opt. Lett.*, vol. 44, no. 16, pp. 4052–4055, Aug. 2019.

[15] W. Hao, Y. Dai, F. Yin, Y. Zhou, J. Li, J. Dai, W. Li, and K. Xu, "Chirped-pulse-based broadband RF channelization implemented by a mode-locked laser and dispersion," *Opt. Lett.*, vol. 42, no. 24, pp. 5234–5237, Dec. 2017.

[16] C. X. Xie, D. Zhu, W. J. Chen, J. Liu, and S. L. Pan, "Microwave channelizer based on polarization multiplexing and photonic image-reject mixing," in *Proc. Int. Top. Meeting Microw. Photon.*, Ottawa, ON, Canada, Oct. 2019.

[17] D. Zhu, W. Chen, and S. Pan, "Photonics-enabled balanced Hartley architecture for broadband image-reject microwave mixing," *Opt. Express*, vol. 26, no. 21, pp. 28022–28029, Oct. 2018.

[18] Y. Wang, D. Zhang, B. Xu, Z. Dong, J. Pei, and S. Xu, "T-typed photonic crystal circulator with square lattice Al_2O_3 rods array and NiZn-ferrite posts," *Mater. Des.*, vol. 181, Nov. 2019, Art. no. 107978.

[19] D. Marpaung, C. Roeloffzen, R. Heideman, A. Leinse, S. Sales, and J. Capmany, "Integrated microwave photonics," *Nature Photon.*, vol. 7, no. 4, pp. 506–538, Jul. 2013.

CHENXU XIE received the B.S. degree in information engineering from the Nanjing University of Aeronautics and Astronautics, Nanjing, China, in 2017, where he is currently pursuing the master's degree with the Key Laboratory of Radar Imaging and Microwave Photonics, Ministry of Education. His main research interest includes photonic signal processing.

DAN ZHU (M'12) received the B.S. and Ph.D. degrees in electronic engineering from Tsinghua University, Beijing, China, in 2004 and 2009, respectively.

In July 2009, she joined the Research Department of Radar Signal Processing, No. 14 Research Institute, China Electronics Technology Group Corporation, as a Researcher. In May 2011, she joined the Key Laboratory of Radar Imaging and Microwave Photonics, Ministry of Education, Nanjing University of Aeronautics and Astronautics, Nanjing, China, where she is currently an Associate Professor. Her current research interests include photonic signal processing and the system applications. She is a member of the IEEE Microwave Theory and Techniques Society, the IEEE Photonics Society, and a member of the Optical Society of America.

WENJUAN CHEN received the B.S. degree in electronic science and technology from the Nanjing University of Aeronautics and Astronautics, Nanjing, China, in 2016, where she is currently pursuing the Ph.D. degree with the Key Laboratory of Radar Imaging and Microwave Photonics, Ministry of Education.

Her research interests include photonic signal processing and photonics-based RF front-end.

SHILONG PAN (S'06–M'09–SM'13) received the B.S. and Ph.D. degrees in electronic engineering from Tsinghua University, Beijing, China, in 2004 and 2008, respectively.

From 2008 to 2010, he was a "Vision 2010" Postdoctoral Research Fellow at the Microwave Photonics Research Laboratory, University of Ottawa, Canada. He joined the College of Electronic and Information Engineering, Nanjing University of Aeronautics and Astronautics, China, in 2010, where he is currently a Full Professor and also an Executive Director of the Key Laboratory of Radar Imaging and Microwave Photonics, the Ministry of Education. His research has focused on microwave photonics, which includes optical generation and processing of microwave signals, analog photonic links, photonic microwave measurement, and integrated microwave photonics. He has authored or coauthored over 420 research articles, including more than 230 articles in peer-reviewed journals and 190 papers in conference proceedings.

Prof. Pan is a Fellow of the SPIE and IET, and a Senior Member of the OSA. He is a Steering Committee Member of the IEEE International Topical Meeting on Microwave Photonics, and the International Conference on Optical Communications and Networks. He has also served as the Chair for a number of international conferences, symposia, and workshops, including the TPC Chair for the International Conference on Optical Communications and Networks, in 2015, and the TPC Co-Chair for the IEEE International Topical Meeting on Microwave Photonics, in 2017. He was selected to receive the IEEE Photonics Society Distinguished Lecturer Award, in 2019, an OSA Outstanding Reviewer Award, in 2015, a Top Reviewer of the IEEE/OSA *Journal of Lightwave Technology*, in 2016 and 2018, respectively, and two Publons Peer Reviewer Awards, in 2018. He was awarded the Scientific and Technological Innovation Leading Talents Award of the National Ten Thousand Plan, in 2018. He is currently an Associate Editor of the *Electronics Letters*, a Topical Editor of the *Chinese Optics Letters*, and is a Technical Committee Member of the IEEE MTT-3 Microwave Photonics.